PERGAMON

Renewable Energy 19 (2000) 597–615

RENEWABLE ENERGY

www.elsevier.com/locate/renene

Data bank

Studying the extinction coefficient due to aerosol particles at different spectral bands in some regions at great Cairo

M.A. Mosalam Shaltout[a,*], M.T.Y. Tadros[b], M. El-Metwally[c]

[a]*National Research Institute of Astronomy and Geophysics, Helwan, Cairo, Egypt*
[b]*Faculty of Science, Physics Department, Mansoura University, Egypt*
[c]*The Egyptian Meteorological Authority, PO Box 11784, Cairo, Egypt*

Received 18 June 1998; accepted 8 April 1999

Abstract

Extinction coefficient due to aerosol has been estimated by Pyrheliometric and Gorgie type Actinometric measurements in the industrial, urban areas and compared with agricultural areas. The measurements distributed over one year from June 1992 to May 1993 were made under clear sky for five spectral bands. The results show two maxima in hot wet and spring months and minimum in winter months, but there is a fluctuation in urban area. Diurnal variations show maximum at noon especially in the industrial area. Level of extinction coefficient in the industrial and urban area is greater than that of the agricultural area, except for hot wet months is due to the increase of water vapor content in agricultural area. Spectral distribution of the extinction coefficient decreases monotonically with wavelength. Size of particles in industrial area is greater than in urban and agricultural areas. The temperature and water vapor content have important rules in increasing the extinction coefficient of aerosols.

* Corresponding author. Tel.: +20-2-263-0833; fax: +20-2-554-8020.
E-mail address: mamshaltout@frcu.eun.eg (M.A. Mosalam Shaltout)

0960-1481/00/$ - see front matter
PII: S0960-1481(99)00077-4

1. Introduction

Radiation passing through the atmosphere is a subject to be attenuated by absorption and scattering. The absorption is caused by permanent gases and water vapor and occurs predominantly at discrete wavelengths. Molecular and particulate scattering on the other hand occurs at continuous wavelength near ultraviolet, visible and near infrared regions of spectrum.

It is well known that the presence of aerosol particles in the atmosphere has an important effect on the radiative transfer and thus plays an important role in determining climate [15,23]. The measurements of extinction coefficient (optical thickness) of aerosol is one of the useful methods for monitoring aerosols burden.

Knowing the spectral distribution of direct solar irradiate at ground level allows one to compute the spectral extinction coefficients A_{ab} of solar radiation caused by aerosols. It is obvious that if the extinction over path is large, the radiation reaching the instrument became small to be measurable. On the other hand if the extinction is weak, the transmittance of solar radiation is very close to 0.1 [13]. Rizk et al. [17], studied the effect of pollutant aerosols on spectral atmospheric transmissivity in Cairo, National Research Center (NRC) at Giza by Volz sun photometer in period of July 1981–June 1982. They found that the annual loss in solar energy absorption, in case of dust free atmosphere in Cairo , due to pollutant aerosols for each of blue, green and red bands were 37%, 21% and 19%, respectively. The loss in solar energy absorption by gases for the whole year was 21%. Also, radiation loss due to pollutant aerosols is strongly wavelength dependent, where shorter wavelength is being much more seriously affected than longer wavelength. Fine particles caused more than 56% of the average radiation loss, including NO_2 absorption band.

The aerosol optical thickness is varied with spectral bands between the highest value equal to 64% at blue band (440 nm) and decreases with wavelength until it reaches 24% at wavelength (880 nm) [18]. This is because the concentration of the fine particles in the Cairo atmosphere is greater than that of the coarse ones. This gives a strong contrast to conditions in maritime aerosol which have well defined peaks at wavelengths from 890 to 1000 nm.

El-Shazely et al. [6] showed that the temperature, relative humidity and wind speed have an important effect on the extinction of the atmosphere at Qena (Egypt). They concluded that temperature and humidity have the significant role of increasing the aerosol mass concentration and thus the atmospheric extinction. They found that the high wind speed causes the dispersion of the dust from eastern and western desert. Also, the high temperature near the earth's surface gives rise to vertical mixing of the pollutants, which rises the particulate matters buoyancy in the atmosphere. Finally, they found that the relative humidity increase more aerosol particles being to absorb water molecules. This leads to effective in their size distribution and refractive index causing an increase in the extinction coefficient with increasing of the relative humidity.

The spectral distribution of direct-normal irradiance and marine aerosol extinction coefficient were studied by Vaxelair et al. [21]. They found that it

defines a characteristic profile of natural marine aerosols and shows weak extinction at about 0.6 μm. Also, the increasing of extinction in the I.R. region is another particularity of this type of oceanic aerosol, and maximum optical thickness is about 0.07 and 0.08, respectively. In this work the extinction coefficient A_{ab} and transmissivity T_{ab} due to aerosol particles in the atmosphere at different bands will be determined by using the method of Vaxelair et al. [21]. The extinction coefficients will be determined in diurnal, monthly and seasonal variation. Also, the effects of some meteorological parameters on the extinction coefficient will be determined.

2. Experimental work

2.1. Equipment

Two types of instruments measured the solar spectrum: Epply Normal Incidence Pyrheliometer model (NIP); and Georgie type Actinometer (designed in the laboratory of Dr Justus Rosenbergen, Hamburg, 1959). Both instruments were equipped with a filter wheel.

The Egyptian Meteorological Authority calibrated both pieces of apparatus (NIP and Georgie) in April 1991. The accuracy on total direct irradiance was 6.15 mV per langlay minuet. The radiation meters that coupled with these instruments are the instantaneous solar radiation meter model No. 455 with sensitivity of 9.9×10^{-6} V/w m^2 with Epply pyrheliometer and galvanometer with Georgie type actinometer.

2.2. Location

An Epply pyrheliometer was mounted on the roof of the research laboratory in the National Research Institute of Astronomy and Geophysics (NRIAG) in Helwan (29.87°N, 31.33°E rise from M.S.L. about 124 m).

A Georgie type actinometer was mounted on the roof of the Egyptian Meteorological Authority in Abbasyia (30.08°N, 31.28°E rise from M.S.L. about 30 m) and also on the roof of the village school in the agricultural area of Mansoura (31.00°N, 31.45°E rise from M.S.L. about 7 m), which is approximately 140 km from Cairo.

2.3. Filters

The classical broad band pyrheliometry and the more recently introduced sun-photometry, are two types of optical filters which can be used in meteorology. The classical broad band pyrheliometry OG1 (530 nm), RG2 (630 nm) and RG8 (695 nm) are now employed in meteorology for separation of certain spectral regions in the radiation received from the sun and sky.

The Schott glass filters OG1, RG2 and RG8 are from the special types which

have been extensively used in meteorology and are acceptable from WMO. In addition to these three filters, there are another two filters, WG7(290) and GG22(395) which have been used in order to cover the spectral regions near ultraviolet, visible and near infrared. Ideal characteristics of filters are given in Table 1

Angstrom and Drummond [2] show that cut off filters, at the wavelength λ value, are corresponding to 50% of transmission from the internal transmittance, where λ_{c1} and λ_{c2} are the low and high cut off wavelength, respectively. In this study λ_{c1} will be used as in Table 1, where λ_{c1} values vary slightly from one filter to another. Because the irradiance is very low in these spectral regions, and the slight deviation has a little influence on the measurements then the average value of the high cut off wavelength for all filters will be considered as $\lambda_{c2}=2.9$ μm.

To evaluate such measurements, the results must be normalized, taking into account the individual filter characteristics. For this purpose, the so-called filter factor has been defined. It is the ratio of the intensity behind an imaginary filter with unity transmission outside, to the intensity measured with the actual filter. Using a reasonable terrestrial solar spectrum as input, then

$$f=\frac{\sum_{\lambda=(\lambda_{c1})_i}^{(\lambda_{c2})_i} I_\lambda \Delta\lambda}{\sum_{\lambda=0}^{\infty} I_\lambda T_{i\lambda} \Delta\lambda} \tag{1}$$

where I_λ is monochromatic irradiance coming from the source and $T_{i\lambda}$ is monochromatic transmittance for the filter i.

The intensity measured behind the filter is multiplied by the filter factor f. The filter factor is normally determined by comparison with standard filter by using the sun as a source and a pyrheliometer as a detector as in Table 1.

2.4. Data

The measurements for different air mass, under clear sky conditions (nebulosity less than 25%, no clouds near the sun), are carried in three regions, Helwan (as

Table 1
Filter characteristics

No. (j) filters	Old name	Filter reference	Interval bands (μm)	λ_{c1} (μm)	Filter factor f
b_1	WG7	WG295	0.290–0.390	0.290	1.080
b_2	GG22	GG395	0.390–0.530	0.390	1.095
b_3			0.290–0.530		1.080
b_4	OG1	OG530	0.530–0.630	0.530	1.080
b_5	RG2	RG630	0.630–0.695	0.630	1.080
b_6	RG8	RG695	0.695–2.900	0.695	1.080

Table 2
Spectral bands distributed over one year to all regionsHelwan, Abbasyia and Mansoura from June 1992 to May 1993. (*, All regions Helwan, Abbasyia and Mansoura; ., Abbasyia and Mansoura only; H, Helwan only)

	Months											
Bands	J	J	A	S	O	N	D	J	F	M	A	M
b_1				.	.	.	.	.	.	.	.	.
b_2				.	.	.	.	.	.	.	.	.
b_3	*	*	*	H	H	H	H	H	H	H	H	H
b_4	*	*	*	*	*	*	*	*	*	*	*	*
b_5	H	H	H	*	*	*	*	*	*	*	*	*
b_6	H	H	H	*	*	*	*	*	*	*	*	*

industrial area), Abbasyia (as urban area) and Mansoura (as agricultural area), in the period from June 1992 to May 1993.

Table 2 shows spectral bands distributed during the above period.

3. Methodology

Vaxelair et al. [21] shows that Bouguer's law describes extinction of monochromatic beams through a homogeneous medium. Monochromatic direct solar irradiate at ground level is given as:

$$I_\lambda = I_{o\lambda} D T_\lambda \tag{2}$$

where $I_{o\lambda}$ is the extraterrestrial irradiance at the mean earth-sun distance for wavelength λ obtained from Frohlich and Wehrli [7]; D is the correction factor for earth-sun distance given by Spencer [19]; and T_λ is the spectral atmospheric transmittance given by:

$$T_\lambda = T_{R\lambda} T_{o\lambda} T_{w\lambda} T_{\mu\lambda} T_{a\chi} \tag{3}$$

where $T_{R\lambda}$, $T_{o\lambda}$, $T_{w\lambda}$ and $T_{\mu\lambda}$ are the transmittance due to Rayleigh scattering by clear dry air, ozone, water vapor and uniformly mixed gases absorption, respectively, and $T_{a\chi}$ is the transmittance due to the extinction by suspended solid and liquid aerosol particles of about 10^{-3}–10^3 μm in size [3,4,10].

The direct radiation I_λ in Eq. (2) is replaced by $I_{b\lambda}$ for that measured at different spectral bands as in Table 1. Irradiance is I_{fj} defined according to measured irradiance I'_{fj} as in the following:

$$I_{fj} = I'_{fj} C_f f F \tag{4}$$

where F is the reduction earth-sun distance $F = 1/D$; C_f is the correction factor of instrument = 1.124; and f is the filter factor as in Table 1.

For spectral band j the direct irradiance I_{bj} is determined from the irradiance obtained for two consecutive filters:

$$I_{bj} = I_{fj} - I_{f(j+1)} \tag{5}$$

for the band six:

$$I_{b6} = I_{f6}. \tag{6}$$

From Eq. (2), the spectral irradiance in each band can be written as in the following form:

$$I_{bj} = \sum_{(\lambda_{c1})_i}^{(\lambda_{c1})_{i+1}} I_{o\lambda} T^*_{\lambda} T_{a\lambda} \Delta\lambda, \tag{7}$$

$$T^*_{\lambda} = T_{R\lambda} T_{o\lambda} T_{\mu\lambda} T_{w\lambda}. \tag{8}$$

The specific spectral transmittance $T_{a\lambda}$ for the aerosols and for different bands is given from Eq. (7) in the form:

$$(T_{ab})_j = \frac{I_{bj}}{\sum_{(\lambda_{c1})_i}^{(\lambda_{c1})_{i+1}} I_{o\lambda} T^*_{\lambda} \Delta\lambda}. \tag{9}$$

The relation between the specific spectral transmittance and extinction coefficients is given as:

$$(T_{ab})_j = \exp[-(A_{ab})_j M_r] \tag{10}$$

therefore the extinction coefficient for aerosols $(A_{ab})_j$ at different spectral bands is:

$$(A_{ab})_j = -\log(T_{ab})_j M_r^{-1} \tag{11}$$

where the relative air mass is obtained by Dogniaux [5] in the form:

$$M_r = \frac{1 - 0.1H}{\sin\ \gamma + 0.15(\gamma + 3.885)^{-1.253}} \tag{12}$$

where H is the height of the station correct to M.S.L. (m) and γ is the altitude angle of the sun (degrees).

Variation of extinction coefficient $(A_{ab})_j$ and transmittance of aerosols $(T_{ab})_j$ will be studied with wavelength. Vaxelair [20] gave a new method for determination of the specific wavelength for each band by the relation:

$$\bar{\lambda}_j = \frac{\sum_{(\lambda_{c1})_i \lambda_j}^{(\lambda_{c1})_{i+1} \lambda_j} \lambda (I_\lambda)' \Delta\lambda}{\sum_{(\lambda_{c1})_i}^{(\lambda_{c1})_{i+1}} (I_{\lambda)'} \Delta\lambda} \tag{13}$$

where:

$$(I_\lambda)' = I_{o\lambda} T_{R\lambda} T_{o\lambda} T_{\mu\lambda} T_{w\lambda}. \tag{14}$$

For $j = 6$, $(\lambda_{c1})_{i+1}$ is replaced by λ_{c2}. The values of $(I_\lambda)'$ are determined for the mean conditions recorded at the site.

4. Results and discussion

The precipitable water vapour for different regions (Fig. 1) was estimated by using Leckner expression [5]. Attenuation coefficient A_{ab} and transmissivity T_{ab} of aerosols were calculated for different bands b_1, b_2, b_3, b_4, b_5 and b_6 to cover approximately most of solar radiation from near ultraviolet to near infrared. A_a is a good indicator for extinction by aerosols. Monthly mean, diurnal variation to each season were computed and seasonally tabulated.

4.1. Monthly mean extinction coefficient A_{ab} and transmissivity T_{ab}

Monthly mean values of A_{ab}, in Abbasyia and Mansoura, for different bands are given in Fig. 2. There are two maxima at autumn and spring months and a

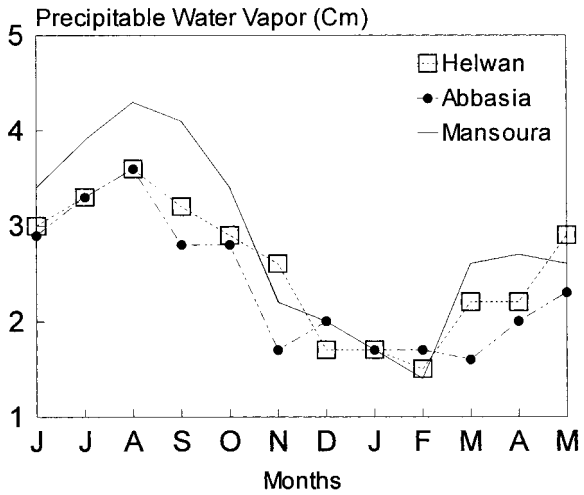

Fig. 1. Precipitable water vapour for different regions.

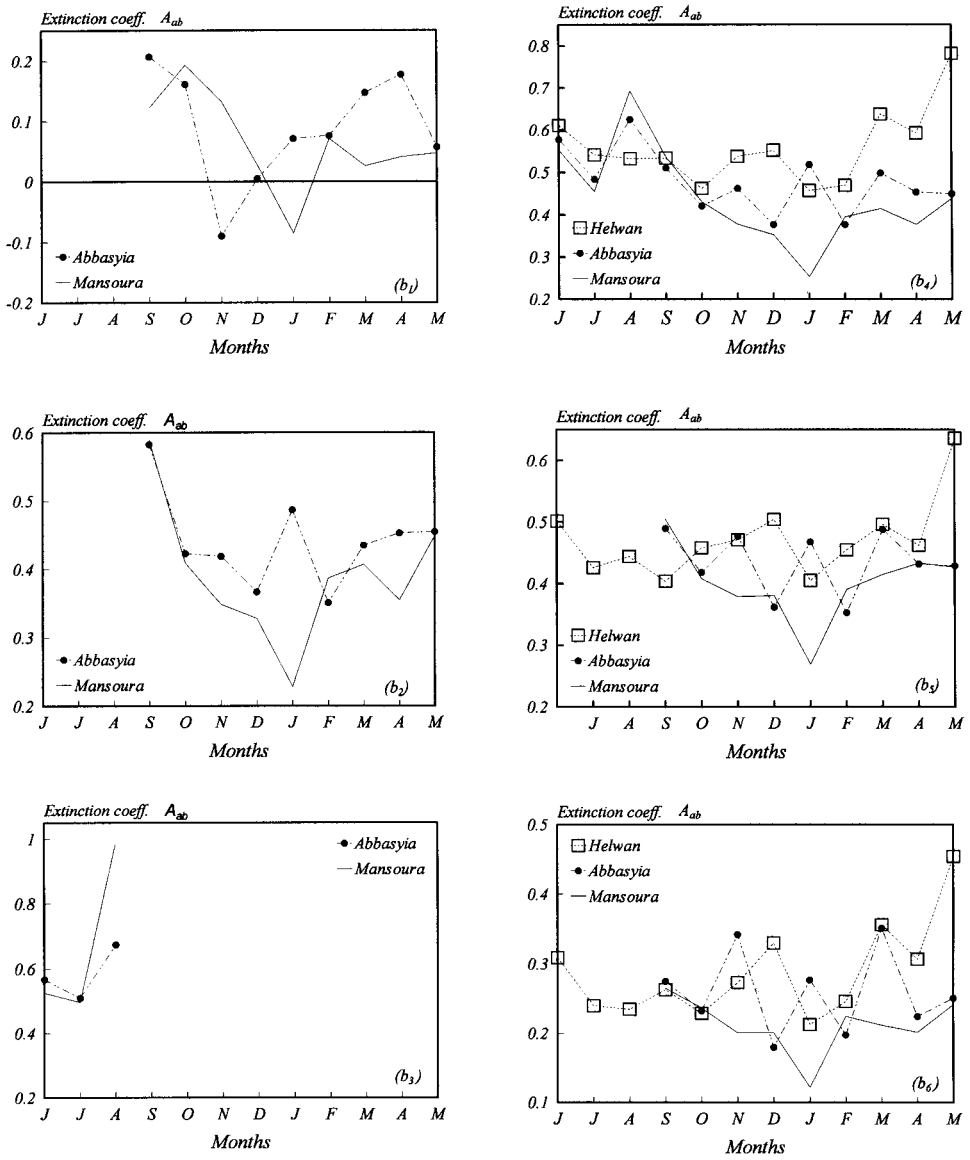

Fig. 2. Monthly mean of extinction coefficient A_{ab} for different bands.

minimum value at winter months as shown for bands b_1 and b_2, with exception for Abbasyia which has a maximum in winter months because of the high stability during these months due to formation of haze and mist most hours of day.

The comparison between the two regions in the above bands show an increase of A_{ab}, in Mansoura than in Abbasyia during autumn months in b_1. But for b_2

the values of A_{ab} in Abbasyia are greater than that for Mansoura during most months due to an increase of aerosol particles.

Monthly mean values in other bands b_4, b_5 and b_6 for the three regions Helwan, Abbasyia and Mansoura are shown in Fig. 2. The values of A_{ab} are high in spring, autumn and approximately high in summer months. This is clear in Helwan and Mansoura, but fluctuated in Abbasyia due to the nature of the urban area. The maximum in summer is appearing clearly in Mansoura and Abbasyia.

Explanation of maximum appearance in summer months in Abbasyia according to Rizk et al. [18], is that due to the low relative humidity, and high day range of surface air temperature result from strong nocturnal radiation specially with weak winds and clear sky. The inversion during night causes low ventilation keeping pollutants suspended in air for times corresponding to their sizes [11,12]. But in Mansoura, the maximum is attributed to increase of water vapor, where the aerosol extinction which derived from multispectral solar flux measurements in the visible and near IR regions increases with increasing atmospheric water vapor [16].

Generally the increase of water content affects the extinction coefficient which may occur in two ways, either by absorption at the particular wavelength or under consideration of the growth of aerosol particles size.

The other maximum that was noticed in the autumn months at Helwan can be attributed to the increase in the emanation of the industry pollutants. The maximum in spring months can be attributed to Khamasin depressions that load the air by dust particles in addition to pollutant particles that already exist especially in Helwan and Abbasyia.

The comparison between regions, as in Tables 3 and 4, shows significant differences between Helwan and Mansoura, during all months, except for summer months, where values of A_{ab} are close to each other. In August A_{ab} values in Mansoura are higher than in Helwan and Abbasyia due to the increase of water content as shown in Fig. 1. This result is logical because of the differences between the industrial region (Helwan) and the agricultural region (Mansoura). But the urban area of Abbasyia fluctuated between them, and its value is close to Mansoura.

The monthly mean of transmissivity T_{ab} as shown in Fig. 3 for different bands is the reverse of the extinction coefficient. Its profile shows two main maxima in summer and spring and secondary maximum in autumn months. This is clear for all bands except b_1, which may be due to the increase in temperature and hence the dispersion of the aerosols [17].

Transmissivity T_{ab} in Mansoura is higher than Helwan but less for Abbasyia in some months, because of low A_{ab} in Mansoura. In autumn months, and in some bands, Mansoura is lower than the remaining regions, this is attributed as mentioned before to the increase of water content.

4.2. Diurnal variation of extinction coefficient A_{ab}

Diurnal variation of A_{ab} for all bands b_1, b_2, b_3, b_4, b_5 and b_6 in all regions is shown in Figs. 4–6. These figures show that the values of A_{ab} are higher at noon

Table 3
Monthly mean of the extinction coefficient A_{ab} and transmissivity T_{ab} due to aerosols for all bands in (a) Helwan, and (b) Abbasyia

Band		J	J	A	S	O	N	D	J	F	M	A	M
(a) For Helwan													
b_3	A_{ab}	0.390	0.244	0.381	0.392	0.262	0.357	0.477	0.318	0.36	0.469	0.410	0.483
	T_{ab}	0.587	0.712	0.569	0.582	0.640	0.545	0.397	0.551	0.554	0.461	0.576	0.483
b_4	A_{ab}	0.561	0.492	0.483	0.484	0.412	0.488	0.502	0.407	0.419	0.588	0.543	0.732
	T_{ab}	0.469	0.515	0.497	0.513	0.490	0.407	0.353	0.431	0.515	0.383	0.481	0.419
b_5	A_{ab}	0.452	0.376	0.394	0.354	0.408	0.421	0.454	0.355	0.405	0.466	0.412	0.586
	T_{ab}	0.542	0.610	0.558	0.610	0.517	0.459	0.388	0.488	0.503	0.488	0.575	0.506
b_6	A_{ab}	0.309	0.240	0.235	0.263	0.229	0.273	0.330	0.213	0.246	0.356	0.307	0.454
	T_{ab}	0.653	0.719	0.698	0.690	0.667	0.590	0.487	0.639	0.653	0.563	0.660	0.593
(b) For Abbasyia													
b_1	A_{ab}				0.207	0.161	−0.090	0.005	0.071	0.076	0.147	0.177	0.057
	T_{ab}				0.839	0.845	1.198	1.202	0.975	0.992	0.876	0.854	0.991
b_2	A_{ab}				0.583	0.423	0.419	0.367	0.487	0.321	0.435	0.453	0.455
	T_{ab}				0.470	0.534	0.480	0.496	0.402	0.580	0.492	0.549	0.563
b_3	A_{ab}	0.517	0.460	0.624									
	T_{ab}	0.514	0.550	0.430									
b_4	A_{ab}	0.528	0.434	0.575	0.461	0.371	0.412	0.327	0.469	0.326	0.449	0.404	0.400
	T_{ab}	0.507	0.567	0.454	0.547	0.575	0.492	0.428	0.419	0.600	0.484	0.584	0.600
b_5	A_{ab}				0.440	0.368	0.427	0.32	0.418	0.303	0.438	0.382	0.379
	T_{ab}				0.561	0.577	0.493	0.543	0.453	0.622	0.509	0.600	0.616
b_6	A_{ab}				0.275	0.233	0.342	0.180	0.277	0.198	0.351	0.225	0.251
	T_{ab}				0.694	0.706	0.554	0.696	0.584	0.734	0.562	0.735	0.723

Table 4
Monthly mean of the extinction coefficient A_{ab} and transmissivity T_{ab} due to aerosols for all bands in Mansoura

Band		J	J	A	S	O	N	D	J	F	M	A	M
b_1	A_{ab}				0.122	0.193	0.133	0.027	−0.085	0.071	0.026	0.041	0.047
	T_{ab}				0.977	0.843	0.957	1.028	1.289	0.957	1.019	0.987	1.000
b_2	A_{ab}				0.589	0.409	0.349	0.328	0.228	0.387	0.407	0.355	0.449
	T_{ab}				0.436	0.486	0.481	0.473	0.629	0.512	0.552	0.619	0.570
b_3	A_{ab}	0.475	0.447	0.934									
	T_{ab}	0.516	0.558	0.315									
b_4	A_{ab}	0.503	0.405	0.643	0.487	0.381	0.328	0.303	0.204	0.345	0.365	0.327	0.389
	T_{ab}	0.497	0.577	0.452	0.503	0.504	0.494	0.495	0.649	0.550	0.588	0.644	0.619
b_5	A_{ab}				0.455	0.358	0.329	0.331	0.219	0.341	0.365	0.383	0.377
	T_{ab}				0.522	0.522	0.490	0.467	0.630	0.554	0.590	0.600	0.624
b_6	A_{ab}				0.265	0.237	0.201	0.201	0.122	0.225	0.212	0.202	0.243
	T_{ab}				0.683	0.646	0.642	0.621	0.767	0.672	0.735	0.759	0.740

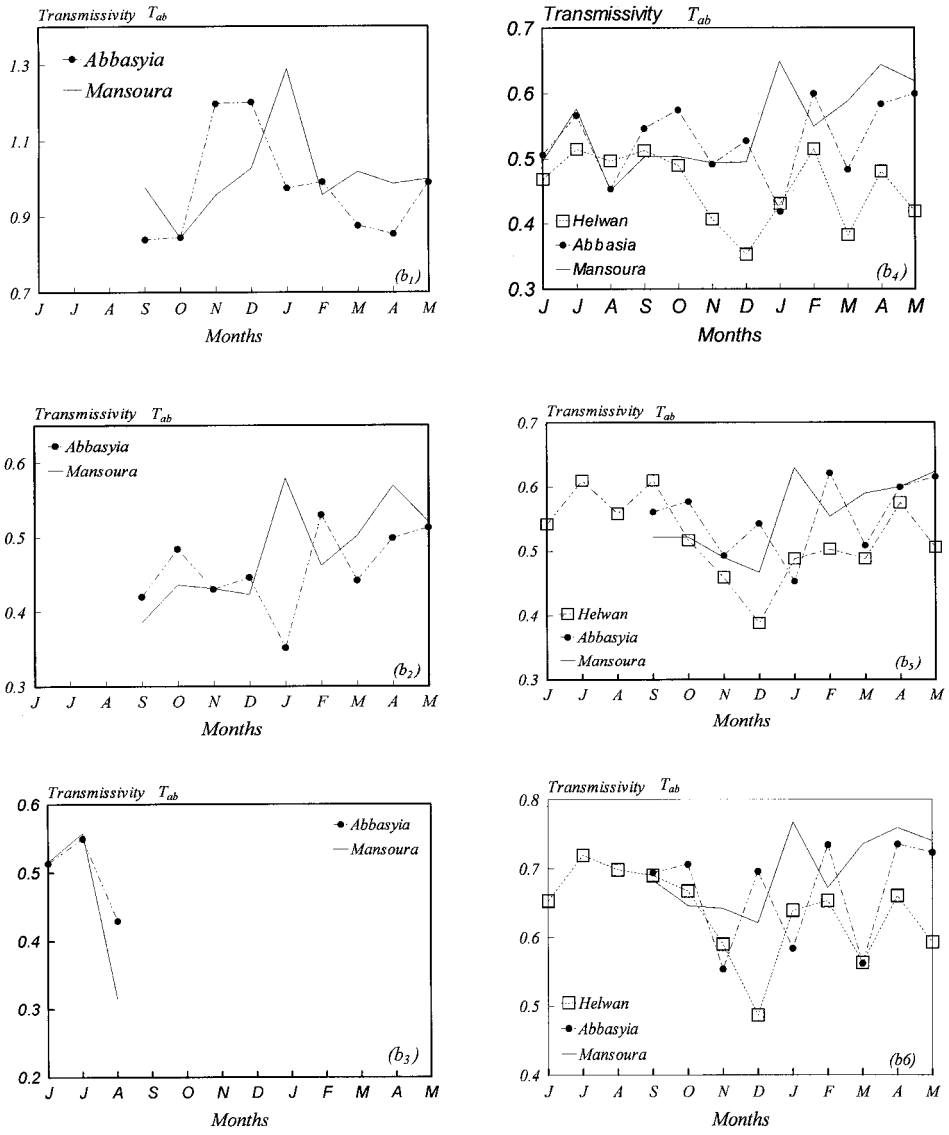

Fig. 3. Monthly mean of transmissivity T_{ab} for different bands.

for all bands in all seasons except in winter and spring at band b_4, which has insignificant variation in Mansoura and Abbasyia. Also, it has high values during the morning in autumn and winter seasons in Abbasyia, and high values for spring in Mansoura.

The higher values of A_{ab} in Abbasyia during the morning can be attributed to

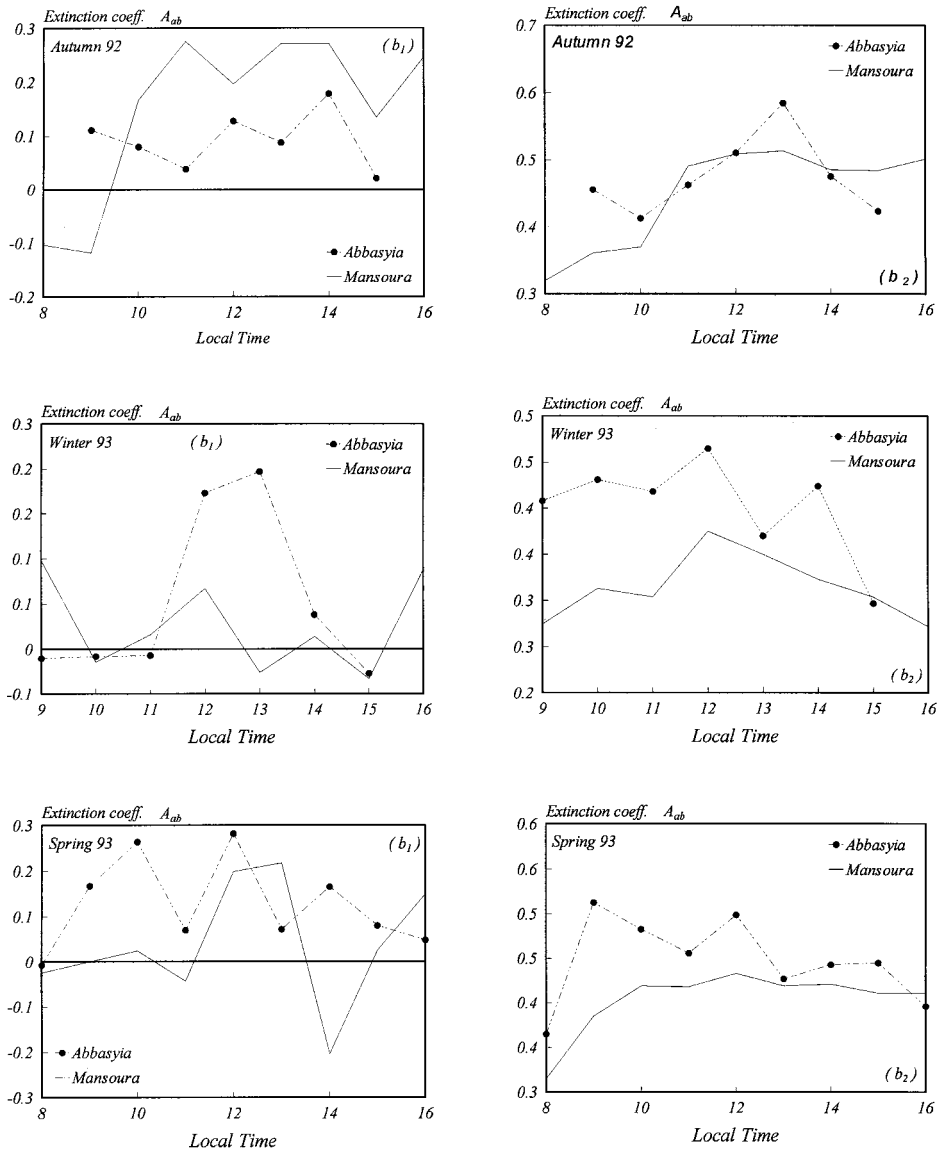

Fig. 4. Diurnal variation of extinction coefficient A_{ab} at different seasons for bands b_1 and b_2.

traffic peaks which result in high concentrations of carbon monoxide, nitrogen oxides, hydrocarbons as well as high levels of lead in the suspended dust. This is because Abbasyia is midway between Shoubra El-Kheima city (which has industrial activity) and Cairo airport. All of these pollutant particles give a chance to photo chemical smog forming under the favorable conditions of gentle wind

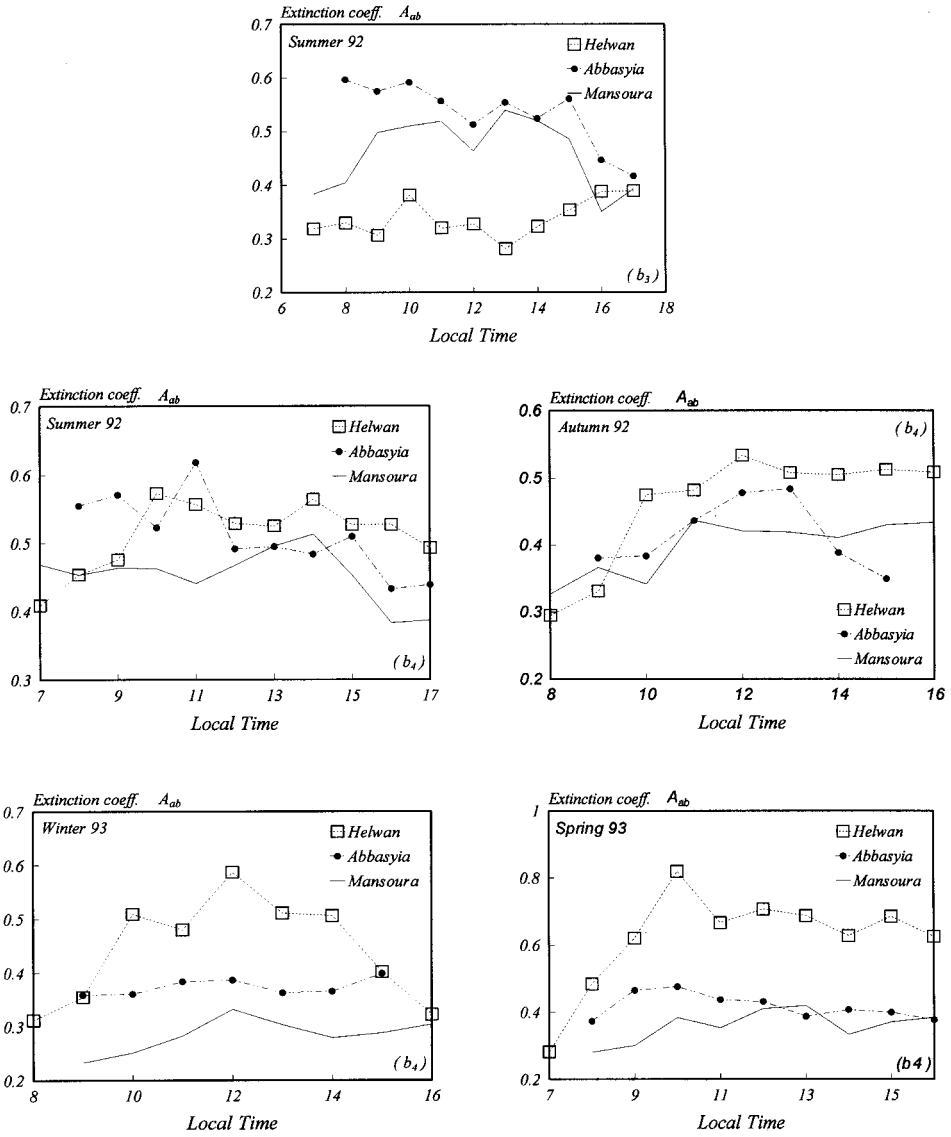

Fig. 5. Diurnal variation of extinction coefficient A_{ab} at different seasons for bands b_3 and b_4.

and moderate to high humidity. The values of A_{ab} are low in the afternoon because of the lower values of relative humidity, which result in decreasing the condensation [17].

High values of A_{ab} at noon for all regions are attributed to a change in temperature that causes evaporation of moisture in the atmosphere [10], and an increase in heating of the atmosphere which causes increasing thermal motion,

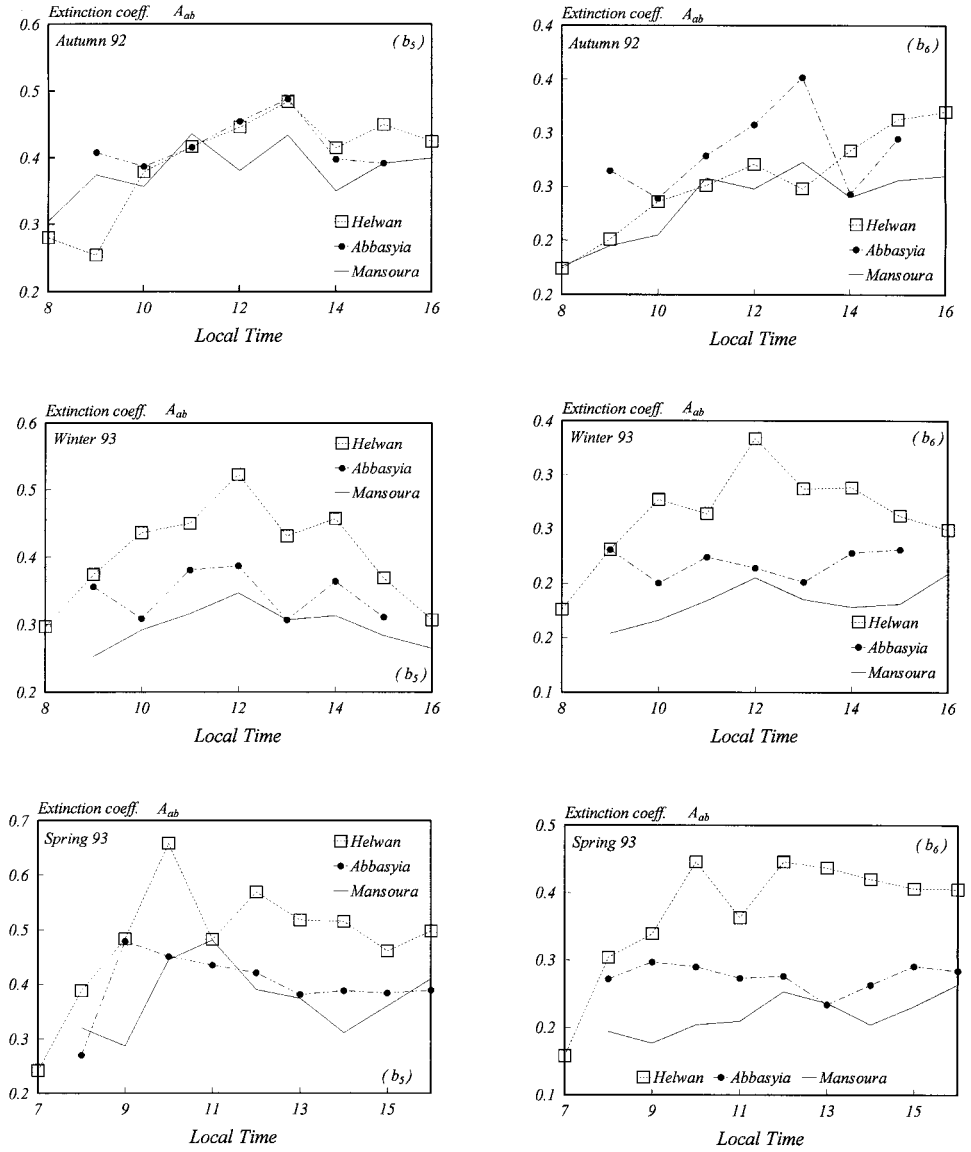

Fig. 6. Diurnal variation of extinction coefficient A_{ab} at different seasons for bands b_5 and b_6.

and the possibility exists that this will lead to rupture of some of the molecular aggregates giving a large number of aerosol particles with smaller radii [1,8]. These changes will result in an increase of A_{ab}, which is much clearer in Helwan because of the spread of cement and steel factories. Mansoura in the afternoon has high values of A_{ab}, due to an increase of water precipitation from evaporation processes of the plants as in Fig. 1.

Table 5
Seasonal mean of the extinction coefficient A_{ab} and transmissivity T_{ab} due to aerosols for different bands in Helwan, Abbasyia and Mansoura regions

		Helwan		Abbasyia		Mansoura	
A_{ab}	T_{ab}	A_{ab}	T_{ab}	A_{ts}	T_{ab}	A_{ab}	T_{ab}
Summer	b_3	0.338	0.623	0.534	0.498	0.461	0.537
	b_4	0.512	0.493	0.512	0.509	0.454	0.537
	b_5	0.404	0.570				
	b_6	0.261	0.690				
Autumn	b_1			0.92	0.961	0.150	0.926
	b_2			0.475	0.495	0.449	0.467
	b_3	0.337	0.589				
	b_4	0.461	0.470	0.415	0.538	0.399	0.500
	b_5	0.395	0.529	0.412	0.543	0.381	0.511
	b_6	0.255	0.649	0.283	0.651	0.234	0.657
Winter	b_1			0.051	1.056	0.004	1.092
	b_2			0.402	0.493	0.314	0.538
	b_3	0.386	0.501				
	b_4	0.443	0.433	0.374	0.516	0.284	0.564
	b_5	0.405	0.460	0.345	0.539	0.297	0.550
	b_6	0.263	0.593	0.218	0.671	0.183	0.686
Spring	b_1			0.127	0.907	0.038	1.002
	b_2			0.448	0.535	0.404	0.581
	b_3	0.522	0.507				
	b_4	0.621	0.428	0.418	0.556	0.360	0.617
	b_5	0.481	0.523	0.400	0.575	0.375	0.605
	b_6	0.372	0.600	0.276	0.673	0.219	0.744
Yearly mean	b_1			0.090	0.975	0.064	1.010
	b_2			0.442	0.508	0.389	0.529
	b_3	0.396	0.555				
	b_4	0.509	0.456	0.430	0.530	0.374	0.555
	b_5	0.421	0.521	0.386	0.552	0.351	0.555
	b_6	0.288	0.633	0.259	0.665	0.212	0.696

Table 5 shows the seasonal mean of A_{ab} at different bands and different regions. It is clear that Helwan is higher than Abbasyia and Mansoura especially in spring and winter, which are in agreement with the monthly mean.

Generally the results of yearly mean for all bands, (see Table 5), show that A_{ab} values in Helwan are higher than Abbasyia, and those for Abbasyia are higher than Mansoura.

4.3. Variation of extinction coefficient A_{ab} and transmissivity T_{ab} with wavelength

Seasonal mean variation of A_{ab} with the spectral bands for all regions as in Fig. 7, show one maximum at band b_4 ($\bar{\lambda} \cong 0.584$ μm) in Helwan and maximum in Abbasyia at band b_2 ($\bar{\lambda} \cong 0.470$ μm) except in the autumn season which has another maximum at band b_5 ($\bar{\lambda} \cong 0.664$ μm) but Mansoura has two maxima at

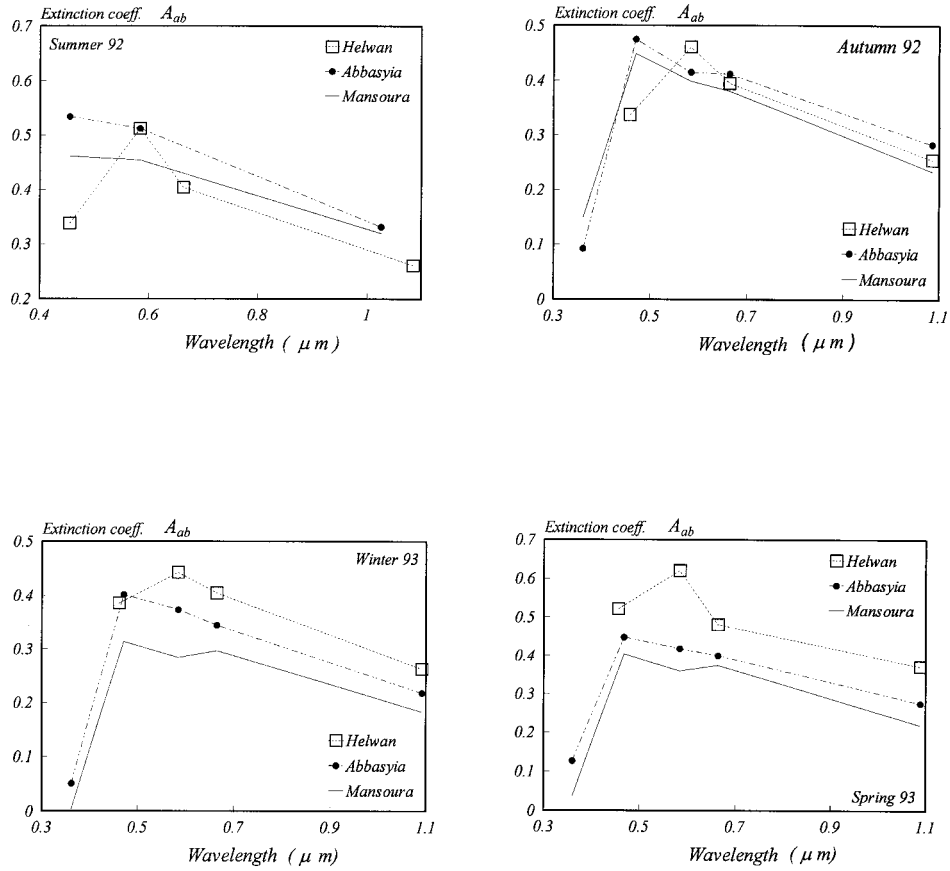

Fig. 7. Spectral distribution of the extinction coefficient A_{ab} due to aerosols for differences at Helwan, Abbasyia and Mansoura.

bands b_2 and b_5. The classical distribution of the aerosol extinction is monotonically decreasing function of wavelength. This is clear in all regions especially in red and near infrared bands [14], where, their studies on dust storm (Khamasin) show maximum at 0.550 μm during measurements in 1971–1973 and at about 0.650 μm on a day in 1977, and minimum at 0.45 μm and at 1 μm. Also, they found that wavelength exponent α is close to zero during above studies, which is an indication for increasing of aerosol particles.

Helwan profile for all seasons presents the same characteristics as above. The extinction emphasizes that Helwan has large size particles, because of the concentration of industrial activities.

The Abbasyia profile has the same characteristics as that obtained by Rizk et al. [18], except for summer season because of lack of band measurements during this period. Rizk et al. [18] found that fine particles in the Cairo atmosphere were in

much more concentration than coarse ones. They noticed that A_{ab} for blue band 0.440 μm had the highest value, then it decreased with increasing wavelength until it reached the lowest value at 0.880 μm.

The results of this work in Abbasyia are also similar in behavior to that of Porto Rico given by Volz [22]. His results for extinction on clear days show higher values at wavelengths 0.430 μm and lower at 1 μm. In Abbasyia it is noticed that there is another little peak in the autumn season at b_5, which reflect that it has large particles with fine particles during this season.

Mansoura has a similar profile of Vaxelair et al. [21], their results were on marine atmosphere, consequently, it has a minimum extinction at about 0.500 μm to 0.600 μm and maximum at about 0.400 μm and into I.R. part of the spectrum. The results of this work in Mansoura differ from their results in I.R. part, but it coincides with results of Rizk et al. [18] in this part.

Generally the increasing population, urbanization and recent industrialization, accompanied by stationary and mobile sources of combustion in Abbasyia, may cause spreading of smoke [9]. The area of such concentration in the atmosphere can affect the extinction of solar radiation. Helwan is highly polluted by large particles, which cause high extinction coefficient A_{ab} which cause the extinction of the solar beam. Consequently it will cause harmful effects on humans, plants and water.

Abbasyia has fine particles, which are in size less than 0.2 μm in radius as they affect the blue band (0.440 μm). These fine particles are more dangerous from the pollution point of view because they stand suspended in the atmosphere for a longer time and are easily carried by wind (long life time) [17]. If they are chemically active, they also have harmful effects on humans, plants and water.

Variation of transmissivity T_{ab} with wavelength as in Fig. 8 indicates that increase of the transmissivity is at near infrared and near ultraviolet bands. This is because of the decrease of extinction coefficients during these bands. But it has low values at visible bands because of highest value of A_{ab}. The comparison between regions shows that Mansoura has a higher value than other regions in winter and spring seasons but that the regions are close to each other in autumn, and T_{ab} in Abbasyia is higher than other regions in summer.

5. Conclusion

Monthly mean of extinction coefficient shows two main maxima, one in hot wet months and another in spring months and minimum in winter months. These are clear in industrial and agricultural areas in Helwan and Mansoura, respectively, but it fluctuates in urban area at Abbasyia.

The first maximum that in hot wet months is due to forming the inversion temperature near ground during night that causes low ventilation, keeping pollutants suspended in air for times corresponding to their sizes in the industrial and urban areas, but in Mansoura it is attributed to increase of water vapor content. The second maximum in spring months is attributed to Khamasin

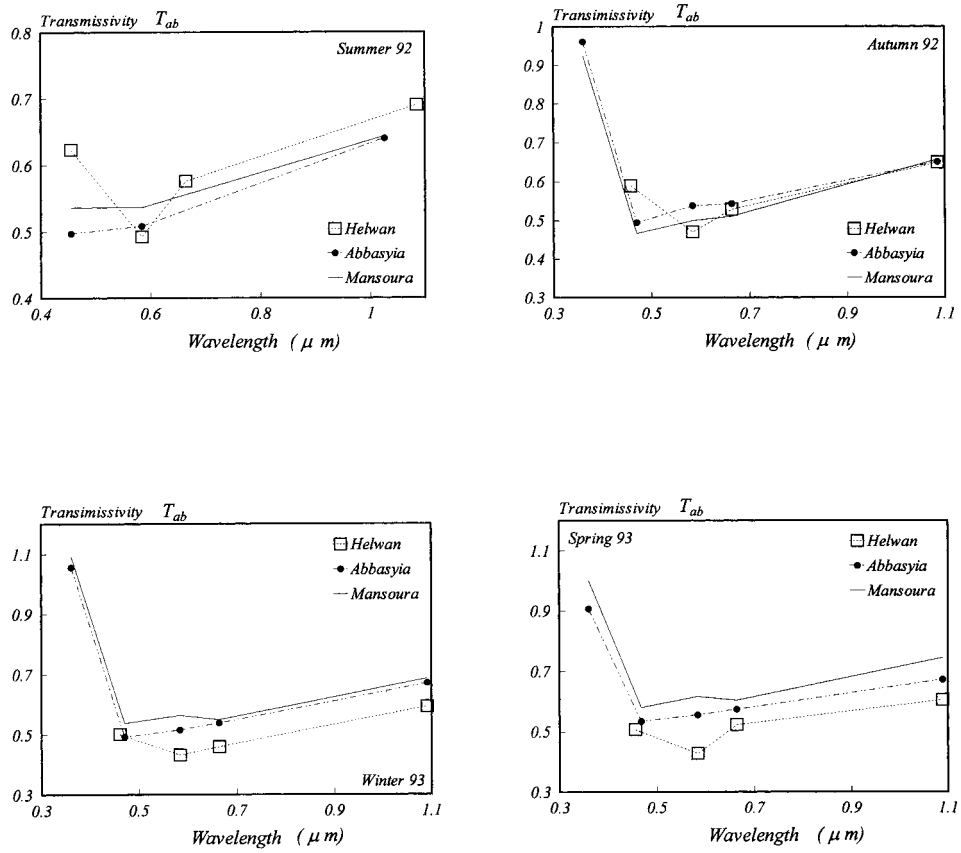

Fig. 8. Spectral distribution of the transmissivity coefficient T_{ab} due to aerosols for differences at Helwan, Abbasyia and Mansoura.

depression that loads the air by dust particles in addition to pollutant particles that already exist.

Otherwise, monthly mean of transmissivity shows reverse behavior to extinction coefficient due to increase of temperature from the dispersion of aerosols in hot wet and spring season.

Transmissivity in Mansoura is larger than polluted areas. It is noticed that A_{ab} increases at noon due to increase of thermal motion and the possibility exists that this will lead to the rupture of some of the molecular aggregates giving a large number of aerosol particles with smaller radii.

The spectral distribution of extinction coefficient by aerosols is a monotonically decreasing function of wavelength. Helwan and Abbasyia profiles show maximum at 0.550 μm and 0.470 μm, respectively. This emphasizes that Helwan has large

size particles because of the increase of industrial activity especially cement and steel factories.

References

[1] Abdelrahman MA, Said SA, Shuaib AN. Comparison between atmospheric turbidity coefficients of desert and temperate climates. J Sol Energy 1988;40:219–25.
[2] Angstrom AK, Drummond AJ. Transmission of (cut-off) glass filters employed in solar radiation research. I J Optic Soc Amer 1959;49:1096–9.
[3] Bird RE, Riordan C. Simple solar spectral model for direct and diffuse irradiance on horizontal and tilted planes at the earth's surface for cloudless atmosphere. J Climate Appl Met 1986;25:87–97.
[4] Brunberger H, Stein RS, Powell R. In: Light scattering, science and technology, 1986. p. 38.
[5] Dogniaux R. Computer procedure for account calculation of radiation data related to solar energy utilization. Proceedings of the Unesco/WMO Symposium 1977;477:191–7.
[6] El-Shazely SM, Abdelmaged AM, Hassan GY, Nobi B. Atmospheric extinction related to aerosol mass concentration and meteorological condition in the atmosphere of Qena (Egypt). Mausam 1991;42:367–74.
[7] Frohlich C, Wehrli C. Spectral distribution of solar irradiance from 25000 nm to 250 nm. World radiation center, Davos, Switzerland, 1981.
[8] Hansen V. Determination of atmospheric turbidity parameters from spectral solar radiation measurements. Arch Met Geoph Biokl Ser B 1974;22:301–8.
[9] Higazy NA. Effect of air pollution visibility and penetration of solar ultraviolet radiation. Ph.D. thesis, Cairo University, 1976.
[10] Iqbal M. An introduction to solar radiation. Academic Press, 1983.
[11] Kambezidis HD, Founda DH, Papanikolaou NS. Linke Unsworth-Monteith turbidity parameters in Athens. Q J R Meteor Soc 1993;119:367–74.
[12] Kobayashi T, Yano N. Relation between observed aerosol optical thicknesses and calculated values from size distribution measurements. J Met Soc Japan 1982;60:1249–58.
[13] Lenoble J. Atmospheric radiative transfer. Hampton, VA: Deepak, 1993.
[14] Levin Z, Joseph J, Mekler Y. Properties of sharav (Khamasin) dust-comparison of optical and direct sampling data. J Atm Sci 1980;37:882–91.
[15] Mitchell Jr JM. The effect of atmospheric aerosols on climate with special reference to temperature near the earth's surface. J Appl Met 1971;10:703–14.
[16] Niranjan K, Ramesh Babu Y. Atmospheric water vapor and its effect on aerosol extinction at coastal station-Visakhapatnam. Mausam 1993;44:243–8.
[17] Rizk HFS, Farag SA, Ateia AA. Effect of pollutants on spectral atmospheric transmissivity in Cairo. Environ Int 1985;11:487–92.
[18] Rizk HFS, Soliman SH, El-Beialy AB, Ateia AA. Aerosol optical thickness in Cairo. J Inst Engineers 1986;66:45–51.
[19] Spencer JM. Fourier series representation of the position of the sun. Search 1971;2:172.
[20] Vaxelair P. Etude de la reparition spectrale du rayonnement solair au sol. à lile de la réunion. Thése de Doctorat Universite Paris VII, Paris, 1989.
[21] Vaxelair P, Leveau J, Mengy G, Baldy S. Ground-level spectral distribution of solar direct-normal irradiance and marine aerosol attenuation coefficient at Reunion Island. Sol Energy 1991;47:189–96.
[22] Volz FE. Spectral skylight and solar radiation measurements in the Caribbean: maritime aerosols and Sahara dust. J Atm Sci 1970;27:1041–7.
[23] Yamamoto G, Tanaka M. Increase of global albedo due to air pollution. J Atm Sci 1972;8:1405–14.